MADRID
inter.noise 2019
June 16 - 19
NOISE CONTROL FOR A BETTER ENVIRONMENT

Research on acoustic characteristics of a regular fluctuate deformed sphere

Peng, Xirui[1], Chen, Zhigang, He Daqian, Miao Tiancheng
National Key Laboratory on Ship Vibration and Noise, China Ship Development and Design Center
No.268, Road ZhangZhidong, Wuhan, China.

ABSTRACT

Acoustic characteristics of a regular fluctuant deformed sphere including its derived models in water is studied by using the planar elements method for forecasting echo characteristics of sonar targets. The effects of surface corrugation's height, period, frequency and azimuth angle of incident plane wave on the spatial distribution and frequency response characteristics of acoustic target strength are analyzed. The mechanism of the formation of spatial distribution characteristics of target strength in different frequency bands and different angles is discussed. The spatial distribution and frequency response characteristics of the target strength of the 3D printed regular fluctuant deformed nylon sphere is measured in acoustic tank, which are in good agreement with the theoretical computed results. Understanding and grasping the acoustic scattering characteristics of regular fluctuant deformed sphere is helpful to carry out research on controlling the scattering acoustic field by using the acoustic metamaterials.

Keywords: Fluctuant deformed, Target Strength, Acoustic metamaterials
I-INCE Classification of Subject Number: 76

1. INTRODUCTION

Study on acoustic scattering of a rough surface is a matter with theoretical and practical significance[1]. Echo characteristics of a rough surface can be applied to medical ultrasound, ultrasonic non-destructive testing and so on. A long-time research on acoustic scattering of rough surface which almost are based on acoustic scattering of fluctuate seabed and sea surface[2-4] were started by Lord Rayleigh. The rough surface is assumed to be a random fluctuate plane which satisfies with Gaussian distribution. The research methods include Kirchhoff approximation, perturbation method based on Rayleigh assumption, integral equation method and small slope approximation. There are many scholars started study aimed at acoustic scattering of underwater rough surface target. The null filed approach was elicited by P.Jansson based on Helmholtz integral equation .Acoustic scattering characteristics of random rough surface spherical target based on Gaussian distribution was studied by him[5].

[1] asally219@126.com

Target made up of deterministic regular corrugation (including sine corrugation and sine-squared corrugation) surface is a particular case of random rough surface. Whatever the degree and the slope of surface fluctuation is, its scattering sound field is always relevant, which leads to an intensive study on acoustic scattering of a rough surface. Acoustic scattering time-domain feature of pulse waveforms of wide band of rigid sphere and cylinder with sine-square corrugation fluctuation is investigated by using mixed method of Kirchhoff/diffraction[6]. In recent years, however, research on acoustic scattering characteristics of underwater surface with regular corrugation is rare.

Target echo characteristics of underwater solid sphere with regular corrugation (sine-squared curve) surface (rigid and non-rigid) is investigated by using the planar elements method (based on Kirchhoff approximation) for forecasting echo characteristics of sonar targets. The effects of surface corrugation's height, period, frequency and azimuth angle of incident plane wave on the spatial distribution and frequency response characteristics of acoustic target strength are analyzed. The mechanism of the formation of spatial distribution characteristics of target strength in different frequency bands and different angles is discussed. The spatial distribution and frequency response characteristics of the target strength of the 3D printed regular fluctuant deformed nylon sphere is measured in acoustic tank.

2. REGULAR FLUCTUANT DEFORMED SPHERE

The 3-dimensional regular fluctuant deformed sphere rotated from the sine-square corrugation curve satisfied with the Equation (1) in x-y plane is seen as an typical target to study. Its surface equation is displayed in Equation (2).

$$r(R,\varphi)=R\left(1-\xi\sin^2(n\varphi)\right),\quad n=0,1,2\cdots \tag{1}$$

$$\begin{cases} x(R,\theta,\varphi)=r(R,\varphi)\cos(\varphi)\cos(\theta) \\ y(R,\theta,\varphi)=r(R,\varphi)\sin(\varphi)\cos(\theta) \\ z(R,\theta,\varphi)=r(R,\varphi)\sin(\theta) \end{cases} \tag{2}$$

In these equations, R is external radius of the sphere. ξ is the ratio of corrugation fluctuant height h to external radius R, $\xi=2h/R$. n is the number of corrugation periods in the range of $(0,\pi)$. θ is glancing angle. φ is azimuth angle. Sine-square corrugation curve (a and c) and three-dimensional rendering fluctuant deformed sphere (b and d) (n=5,8) is shown in figure 1. In this figure, R = 0.3m , ξ=10% ,the dotted line is average curve of corrugation and its radium $R_1=R-h$. We can form a conclusion that average curve equals to the perimeter of corrugation curve via some simple deduction.

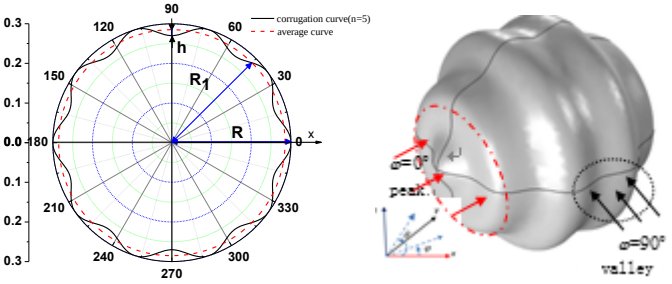

(a) (b)

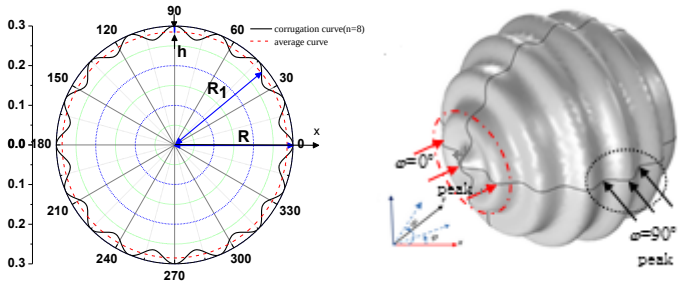

(c) (d)

Figure 1. The sine squared curve（a,c）and three-dimensional rendering of corrugated surface sphere（b,d）

That the fluctuant deformed sphere surface presents 'peaks and valleys' structure can be seen in figure 1. When n is odd, peak structure is presented while azimuth angle φ=0° and valley structure while φ=90°. When n is even, peak structure is presented while azimuth angle φ=0° as well as φ=90°. The arc length of a peak and valley period is shown in Equation 3, which is equivalent to equally divide the length of average curve into 2n parts.

$$\hat{l} = \pi(R-h)/n \tag{3}$$

It is assumed that surface have following two acoustic characteristics[7,8] in compute simulation. Assumption 1 is that the surface is rigid and satisfied with rigid boundary condition described in Equation (4). Assumption 2 is that the surface is non-rigid and satisfied with boundary condition described in Equation (5).

$$\begin{cases} \varphi_i = \varphi_s \\ \dfrac{\partial(\varphi_i + \varphi_s)}{\partial n} = 0 \end{cases} \tag{4}$$

$$\begin{cases} \varphi_s = V(\theta_1)\varphi_i \\ \dfrac{i\omega\rho(\varphi_s + \varphi_i)}{\partial(\varphi_s + \varphi_i)/\partial n} = -Z_n \end{cases} \tag{5}$$

In these equations, φ_i is potential function of incident wave. φ_s is potential function of scattered wave. ω is the circular frequency of incident wave. The density of water is ρ and the velocity c. The density of sphere is ρ_1, longitudinal wave velocity c_l and shear wave velocity c_s. The reflection coefficient of part surface $V(\theta_1)$ is shown in Equation (6)[9,10].

$$V(\theta_1) = \frac{Z_l \cos^2 2\gamma_t + Z_t \sin^2 2\gamma_t - Z}{Z_l \cos^2 2\gamma_t + Z_t \sin^2 2\gamma_t + Z} \tag{6}$$

Z, Z_l, Z_t are acoustic impedance of fluid, longitudinal wave in solid and shear wave in solid as shown in Equation (7).

$$Z = \frac{\rho c}{\cos\theta_1}, Z_l = \frac{\rho_1 c_l}{\cos\alpha_l}, Z_t = \frac{\rho_1 c_t}{\cos\gamma_t} \tag{7}$$

θ_1 is the angle between incident wave and the normal vector of the surface. α_l is the angle of refraction of longitudinal wave and γ_t is of shear wave. Z_n is acoustic impedance of the surface. No matter how complex the surface is, reflection coefficient

of part surface and acoustic impedance of the surface in infinite surface can be combined by Equation (8).

$$Z/Z_n = \left[1-V(\theta_1)\right]/\left[1+V(\theta_1)\right] \tag{8}$$

3. THE PLANAR ELEMENTS METHOD FOR FORECASTING ECHO CHARACTERISTICS OF SONAR TARGETS

The planar elements method, based on Kirchhoff approximate, is a more mature numerical computation method for forecasting medium-high frequency echo characteristics of sonar targets[12]. Backscattering non-rigid target strength of sonar target based on physical acoustic or Kirchhoff approximation is shown in Equation (9).

$$\mathrm{TS} = 20\log\left|-\frac{ik_0}{2\pi}\mathrm{I}\right| \tag{9}$$

$$\text{While}\quad \mathrm{I} = \int_{s_0} e^{2ik_0\vec{\rho}\cdot\vec{r}_0}(\vec{n}_0\cdot\vec{r}_0)V(\theta_1)ds \tag{10}$$

In the Equation (10), $\vec{\rho}_0$ is a vector of surface element to reference point. $\vec{n}_0$ is the unit normal vector of surface element. $\vec{\mathrm{r}}_0$ is a unit vector of receiving point to reference point. $k_0 = \omega/c$ is underwater wave number. $V(\theta_1)$ is the reflectance of part surface. As shown in the Equation (6), the included angle of incident wave and normal vector of the surface is θ_1.

In the planar elements method, firstly, the three-dimensional geometric surface of the target is divided discretely into several complicated space plates, which are replaced by a group of three-dimensional plane plates, usually triangle plates. The sum of all plates' scattering acoustic field is the approximate value of total scattering acoustic field. This method transfers the single three-dimensional plate into part two-dimensional plane. The surface integral in the Equation (10) is transferred into algebraic operation corresponding to the coordinates of the plate accordingly. Seen in the Equation (11), thereby, the computation speed is improved by avoiding surface integral calculation.

$$\mathrm{I} = V(\theta_1)w\sum_{n=1}^{3}\frac{e^{2ik_0(x_nu+y_nv)}(p_{n-1}-p_n)}{(u+p_{n-1}v)(u+p_nv)} \tag{11}$$

In the Equation (11), $p_n = \left(y_{n+1}-y_n\right)/x_{n+1}-x_n$ while $p_0 = \left(y_1-y_3\right)/x_1-x_3$. n is the vertical number of triangular plate. (x_n, y_n) is the vertex coordinates of triangular plate. $\vec{\mathbf{r}}_{01} = u\vec{i}+v\vec{j}+w\vec{k}$ is the vector from launch point to the reference center of the plate. $\theta_1 = \arccos(\mathrm{w})$ is the included angle between plate normal and incident acoustic line.

If the target is divided into M plane plates, the Equation (10) can be turned into Equation(12).

x'_n, y'_n are the vertex coordinate of the ith plate in the two-dimensional plane. $\vec{\mathbf{r}}_{i01} = u'_i\,\vec{i}+v'_i\,\vec{j}+w'_i\,\vec{k}$ is the vector from launch point to reference center of the ith plate. $V(\theta_{1i})$ is the part reflectance. $\theta_{1i} = \arccos(w_i')$ is the angle from the normal of the ith plate to incident acoustic line.

$$\mathrm{I} = \sum_{i=1}^{M}V(\theta_{1i})w_i'\sum_{n=1}^{3}\frac{e^{2ik(x'_nu'_i+y'_nv'_i)}(p_{i(n-1)}-p_{in})}{(u'_i+p_{i(n-1)}v'_i)(u'_i+p_{in}v'_i)} \tag{12}$$

The computation speed of the planar elements method is faster than usual surface integral computation method. The planar elements method is not only appropriate for forecasting distant field and rigid target echo characteristics, but also near field and non-rigid. At present, the planar elements method is relatively widely applied to forecast medium-high frequency echo characteristics of sonar targets [11-14].

In this paper, the planar elements method will be applied to simulating calculation of echo characteristics of a regular fluctuant deformed sphere. The multiple scattering of acoustic wave is ignored in computation because that the deformation of the model is relatively small [15,16].

4. Numerical Calculation And Analysis

Taking sine-squared corrugation sphere as an example, the planar elements method is used for its echo characteristics numerical simulation. The semi-diameter of the sine-squared corrugation sphere is $R = 0.3\text{m}$ in case that the surface of sphere is satisfied with rigid boundary condition.

4.1 TS-frequency response characteristics

The changing curve of TS-frequency under different corrugation height (ξ=10%，5%，2.5%，1%，0%, ξ=0% shows smooth sphere)and incident angle is shown in Figure 2 while (a) shows incident angle φ=0°,(b) φ=90°. The changing curve of TS-frequency under different corrugation period and height is shown in Figure 2 and 3. The external radius of the sphere is 0.3m. Calculated frequency is 100Hz~50kHz while the interval frequency is 100Hz.

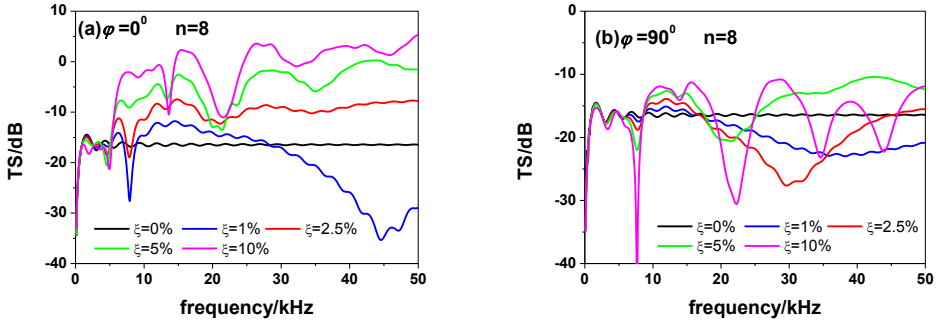

Figure 2. TS-frequency response in under different ξ （a）φ=0°;（b）φ=90°

It is seen from the figure 2 and figure 3 that TS-frequency response of rigid fluctuant deformed sphere in terms of diverse incident angle and diverse fluctuant degree is very different. Generally speaking, TS-low frequency response varying with frequency of the fluctuant deformed sphere with R=0.3m is closed to a sphere. With frequency rising, TS-frequency response of rigid fluctuant deformed sphere gradually deviates from sphere, that is to say corrugation effect of surface gradually influence TS.

Meanwhile, different corrugation fluctuant degree (different ξ) has different influence on TS. With corrugation fluctuant degree increasing (the value of ξ is larger), the influence of corrugation on TS is bigger in terms of medium-high frequency. For example, when φ=0^0， $\xi \geq 2.5\%$, TS varying with frequency increase in terms of medium-high frequency exists a certain fluctuation, but TS increases in total. When φ=90^0, the deviation of fluctuant deformed sphere fluctuation degree of TS from smooth sphere rises with the corrugation fluctuant degree rising.

The main reason of different TS-frequency laws in medium-high frequency with the corrugation fluctuant degree rising between $\varphi=0^0$ and $\varphi=90^0$ is that different sphere surface plays a leading role in different incident angle (Corresponding Fresnel Half-wave zone is different[17]). When incident angle $\varphi=0^0$, peak structure plays a leading role on medium-high frequency scattering. When incident angle $\varphi=90^0$, valley structure plays a leading role on medium-high frequency scattering. As shown in the figure 1(d), the change of TS-frequency response characteristics of different region certainly will present different laws. It is worth noting that TS of fluctuant deformed sphere in medium-high frequency present a certain concussive fluctuation. In addition, the period of concussive fluctuation is smaller and the degree of concussive fluctuation is increased when n and ξ are bigger. The reason of this phenomenon is that with frequency increasing, the incident wave length is smaller while spatial resolution increasing. Under the circumstances, the effect of each strong scattering point or surface gradually emerges. The concussive fluctuation of TS changing with frequency appears because the interference formed by the echo of these strong scattering points. With corrugation fluctuant degree increasing, echo time delay of every strong scattering point increases, which results in smaller period of interference concussion.

4.2 Spatial distribution characteristics of TS

Sine-square fluctuant deformed sphere(ξ =10%， $R=0.3m$)spatial distribution characteristics of TS while n=5 and n=8 are shown in figure 3(a)and 3(b). The calculated frequency are 2kHz, 8kHz, 20kHz.

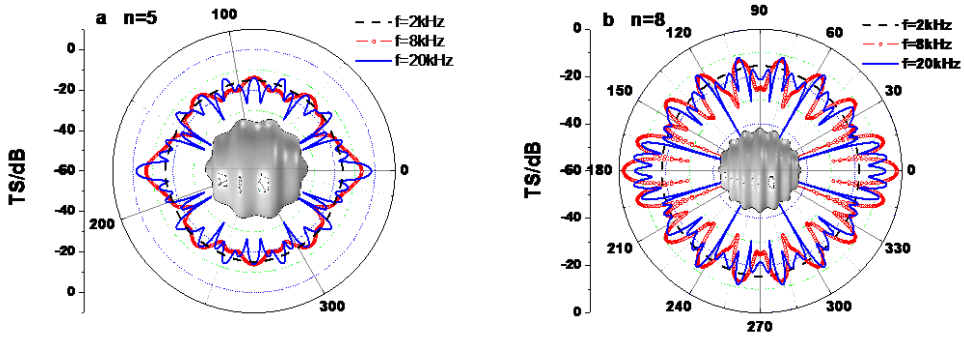

Figure 3. The spatial distribution characteristics of target strength

As shown in the figure 3, fluctuant deformed sphere's spatial distribution characteristics of TS is basically homogeneous and closed to smooth sphere's at low frequency (2kHz). In other words, the corrugation effect doesn't appear. With frequency rising, TS of fluctuant deformed sphere presents 'petaloid' peaks and valleys spatial distribution changing with incident angle and the branch of the 'petaloid' peaks and valleys structure is denser when frequency is higher. Relatively speaking, the 'petaloid' peaks and valleys structure of the n=8 fluctuant deformed sphere is denser than the structure of the n=5 fluctuant deformed sphere.

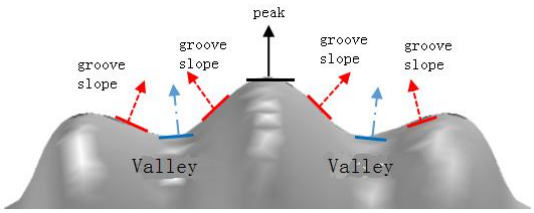

Figure 4. The local structure of corrugated surface

It is worth noting that peaks and valleys of TS 'petaloid' peaks and valleys spatial distribution correspond with peaks and valley structure of fluctuant deformed sphere when frequency rises to frequency band in which the corrugation effect appears. In addition, the branch of TS 'petaloid' peaks and valleys structure corresponds with different surface corrugation structure with frequency rising to different frequency brand. The partial enlarged drawing of n=8 fluctuant deformed sphere is shown in figure 4, in which peak of corrugation (partial specular reflection surface), valley of corrugation (partial specular reflection surface) and groove slope (approximate partial specular reflection surface) are given-that is to say-reflection on fluctuant deformed sphere surface presents characteristics of partial multiple specular reflection in case of medium-high frequency. The main determinant of this phenomena is the analogous degree of wave length λ and arc length of a peak and valley period $\hat{l}$ or fluctuant height $h(\xi)$.At this moment , arc length of a peak and valley period $\hat{l}$ is the main determinant of TS spatial distribution in concerned frequency brand because that little fluctuant corrugation is what we are interested in-that is to say-h, which is corresponding with high frequency, is relatively small while $\hat{l}$,which is corresponding with relatively low frequency is relatively large. Frequency brand partition approximate Equation is deduced according to the following principles. The corrugation effect appears when arc length of a peak and valley period $\bar{l}$ equals to half wave length of incident wave ($\lambda/2$). The approximate Equation of frequency f_e is shown in Equation (13). The peaks and valleys structure can be recognized when arc length of a peak and valley period $\hat{l}$ equals to wave length of incident wave (λ) and the partial multiple specular reflection of peaks and valleys appears. The approximate Equation of frequency f_{fg} is shown in Equation (14). The peaks ,groove slopes and valleys structure can be recognized when arc length of a peak and valley period $\hat{l}$ equals to double wave length of incident wave (2λ) and the partial multiple specular reflection of peaks ,groove slopes and valleys appears. The approximate Equation of frequency f_{fxg} is shown in Equation(15).

$$f_e = cn/\left[2\pi(R-h)\right] \tag{13}$$

$$f_{fg} = cn/\left[\pi(R-h)\right] \tag{14}$$

$$f_{fxg} = 2cn/\left[\pi(R-h)\right] \tag{15}$$

That sine-square fluctuant deformed sphere has partial multiple specular reflection makes its acoustic scattering field multiple peaks structure in the space. This multiple peaks structure is closely related with incident wave frequency and incident angle. The spatial distribution characteristics of acoustic scattering field can be regulated and controlled by adjust period of surface corrugation and fluctuant degree.

5. ACOUSTIC SCATTERING EXPERIMENT

5.1 Experimental layout

This experiment is performed in Shanghai Jiao Tong University hydro-acoustic engineering laboratory water channel. The spatial size of the water channel is $2\text{m}\times1.8\text{m}\times2\text{m}$. The distinction between transducer and hydrophone is $r_1=15.6\text{cm}$ and the distinction between target and hydrophone is $r_2=21.5\text{cm}$. The center of transducer, hydrophone and target are in line and the distance of them to water surface is 1m while

the peak structure (shown in figure 1, 0 °) of target faces the transducer. Emission signal is linear frequency modulation signal. In addition, frequency band includes 60kHz-120kHz and 120kHz-240kHz. The pulse width is 0.01ms. The experimental model is printed by three-dimensional printer and the material of it is nylon. The size of experimental model is as follow: R=0.03m, ξ=10% , $n=8$. Sketch of the experimental layout and photo of experimental model are shown in figure 5.

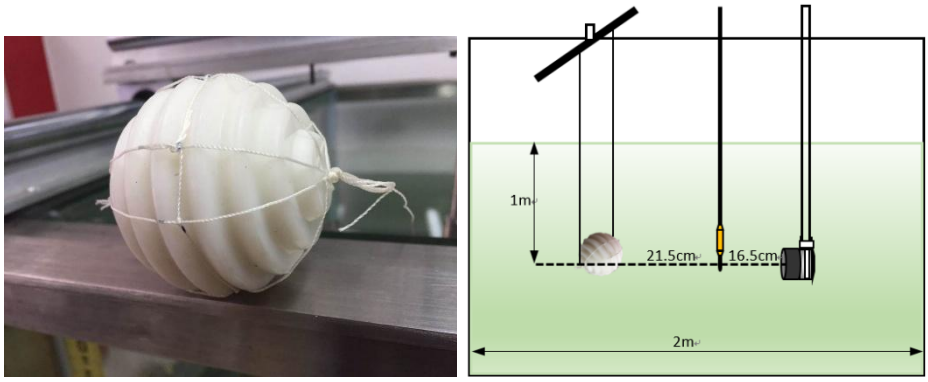

Figure 5. Arrangement of acoustic scattering experiment and model

5.2 Analysis of experimental data

The material parameters of numerical calculation is shown as follow. Density is ρ_1 =1150 kg/m^3. Longitudinal wave velocity is C_d =2680 m/s. Shear wave velocity is C_t =1010 m/s. Water parameters of numerical calculation is shown as follow. Water density is ρ =1000 kg/m^3. Water acoustic velocity is c=1500 m/s.

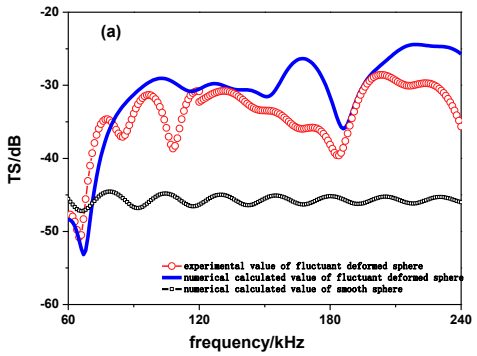

Figure 6. The comparison of experimental and numerical calculation

Curve of TS-frequency when azimuthal angel φ=0^o is shown in figure 6and TS changes with frequency in a fluctuant line. The blue curve is calculated value of fluctuant deformed sphere while the red one is experimental value. The black curve is calculated value of smooth sphere .When frequency is low (60kHz-150kHz), the red curve is consistent with the blue one. When frequency is greater than 150kHz, calculation value is greater than experimental value because of experimental model's material energy absorption which is not considered in calculation. Generally speaking, TS of fluctuant deformed sphere is greater than smooth sphere and is about 10dB averagely.

6. CONCLUSION

Echo characteristics of underwater regular fluctuant deformed (sine-square curve corrugation) sphere incident by plane wave is studied by numerical computation of the planar elements method and experiment. The results show that corrugation's height and period basically have no influence on TS at low frequency. With frequency going up, influence of multiple specular reflection (peaks, groove slopes and valleys) clearly appears. In addition, with corrugation's height and period larger, the fluctuation of TS is larger and the crest value is denser. TS-frequency response characteristics of regular fluctuant deformed nylon sphere printed by three-dimensional printer is measured through flume experiment. The experimental value is consistent with numerical calculation value. Grasping echo characteristics of regular fluctuant deformed sphere is conducive to carry out research of regulating and controlling acoustic scattering field by using acoustic metamaterials.

7. REFERENCES

1. J.A. Ogilvy. "*Theory of Wave Scattering from Random Rough Surfaces*", .Hilger (1991)
2. D. R. Jackson, M. D. Richardson. "*High-Frequency Seafloor Acoustics*", Springer (2007)
3. P. J. Welton. "*Three dimensional analyses of scattering by pressure release sinusoidal surface*", J. Acoust. Soc. Am (2012)
4. Youngmin Choo, H. C. Song, Woojae Seong. "*Numerical study of three-dimensional sound reflection from corrugated surface waves*", J. Acoust. Soc. Am (2016)
5. P. Jansson. "*Acoustic scattering from a rough sphere*", J. Acoust. Soc. Am (1993)
6. J. A. Fawcett. "*Modeling of high-frequency scattering from objects using a hybrid Kirchhoff/diffraction*", J. Acoust. Soc. Am (2001)
7. FAN J,TANG WL,ZHUO LK. "*Planar elements method for forecasting the echo characteristics from sonar targets*", Journal of Ship Mechanics (2012).
8. TANG WL. "*Calculation of acoustic scattering of a non-rigid surface using physical acoustic method*", ACTA ACUSTICA (1993)
9. Brekhovskikh.L. "*Wave in layered medium*", Science Press (1960).
10. Fan J, Zhu BL, Tang WL. "*Modified geometrical highlight model of echoes from non-rigid surface sonar target*", ACTA ACUSTICA (2000)
11. DENG W, FAN J. "*Research on target echo characteristics in torpedo guidance trajectory*", Technical Acoustic (2014)
12. BU KY,FAN J. "*Acoustic image of bright spots of near-field underwater targets based on multi-beam system*", Technical Acoustic (2007)
13. WANG EQ,ZHUO LK,WANG KH. "*High-frequency echo characteristics of single and double shell submarine*", Technical Acoustic (2012)
14. WANG RH,LI B,WEI Q. "*A method for predicting far-field target strength of surface ship based on planar elements theory*", Technical Acoustic (2015)
15. ZHENG GY,FAN J,TANG WL. "*A modified planar elements method considering occlusion and secondary scattering*", ACTA ACUSTICA (2011)
16. ZHANG Y,LI GJ,WANG ZS,JIA B. "*An improved plate element sheltering algorithm*", Technical Acoustic (2016)
17. LIU BS,LEI JY. "*The theory of hydro acoustics*", Harbin engineering university Press (1993)